

# Orthogonal polarization spectral imaging: A new method for study of the microcirculation

WARREN GRONER<sup>1</sup>, JAMES W. WINKELMAN<sup>2</sup>, ANTHONY G. HARRIS<sup>3</sup>, CAN INCE<sup>4</sup>,  
GERRIT J. BOUMA<sup>5</sup>, KONRAD MESSMER<sup>3</sup> & RICHARD G. NADEAU<sup>1</sup>

<sup>1</sup>Cytometrics, Inc., 615 Chestnut Street, Philadelphia, Pennsylvania 19106, USA

<sup>2</sup>Brigham and Women's Hospital, Harvard Medical School, 75 Francis Street, Boston, Massachusetts 02115, USA

<sup>3</sup>Institute for Surgical Research, Klinikum Grosshadern, University of Munich,  
Marchioninistrasse 15, 81377 Munich, Germany

<sup>4</sup>Department of Anesthesiology, Academic Medical Center, University of Amsterdam, Meibergdreef 9,  
1105 AZ Amsterdam, The Netherlands

<sup>5</sup>Department of Neurosurgery, Academic Medical Center, University of Amsterdam, Meibergdreef 9,  
1105 AZ Amsterdam, The Netherlands

Correspondence should be addressed to R.G.N.; email: nadeau@cytometrics.com

Different disease states, including diabetes, hypertension and coronary heart disease, produce distinctive microvascular pathologies. So far, imaging of the human microcirculation has been limited to vascular beds in which the vessels are visible and close to the surface (for example, nailfold, conjunctiva). We report here on orthogonal polarization spectral (OPS) imaging, a new method for imaging the microcirculation using reflected light that allows imaging of the microcirculation noninvasively through mucus membranes and on the surface of solid organs. In OPS imaging, the tissue is illuminated with linearly polarized light and imaged through a polarizer oriented orthogonal to the plane of the illuminating light. Only depolarized photons scattered in the tissue contribute to the image. The optical response of OPS imaging is linear and can be used for reflection spectrophotometry over the wide range of optical density typically achieved by transmission spectrophotometry. A comparison of fluorescence intravital microscopy with OPS imaging in the hamster demonstrated equivalence in measured physiological parameters under control conditions and after ischemic injury. OPS imaging produced high-contrast microvascular images in people from sublingual sites and the brain surface that appear as in transillumination. The technology can be implemented in a small optical probe, providing a convenient method for intravital microscopy on otherwise inaccessible sites and organs in the awake subject or during surgery for research and for clinical diagnostic applications.

At present, the use of microvascular imaging in diagnosis and treatment of human disease is limited. Use has been made of nailfold capillaroscopy in the diagnosis and treatment of peripheral vascular diseases, diabetes and hematological disorders<sup>1-3</sup>. Problems with movement have restricted the use of the bulbar conjunctiva for clinical applications in ophthalmology<sup>4-6</sup>. Other locations observed by intravital microscopy include the microcirculation of the skin, lip, gingival tissue and tongue<sup>4</sup>. Laser-scanning confocal imaging is one new technique that does allow reflected light imaging of the microcirculation *in vivo*<sup>7,8</sup>. This method can distinguish between layers of skin and can image microcirculation in the skin. However, images obtained using laser-scanning confocal microscopy can only be collected at a fraction of the normal video rate (up to 16 versus 30 frames/s) and the best microvascular images using this technique require fluorescent labels for contrast enhancement<sup>7</sup>. Direct observation, using conventional methods, of vascular beds of other organs in humans has been prevented by the need for transillumination, fluorescent dyes for contrast enhancement, or by the size of instrumentation required to acquire images, especially during surgery.

## OPS imaging

In OPS imaging, the subject medium is illuminated with light that has been linearly polarized in one plane, while imaging the remitted light through a second polarizer (analyzer) oriented in a plane precisely orthogonal to that of the illumination. The probe

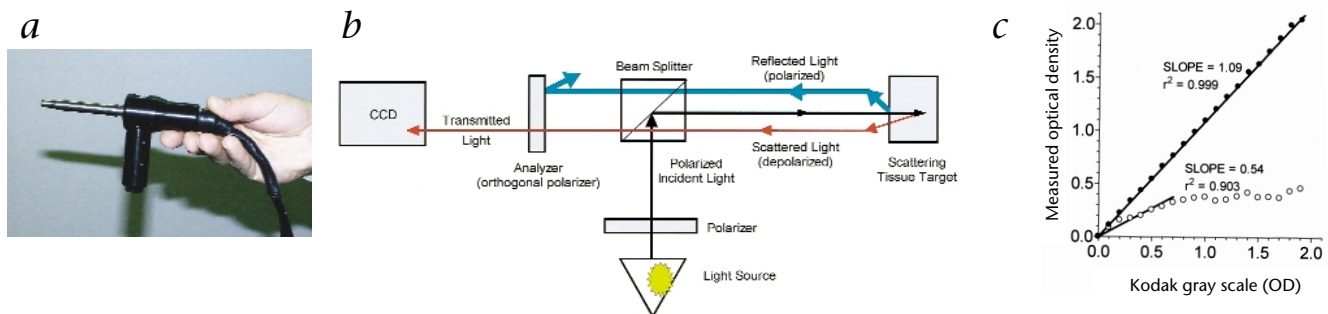
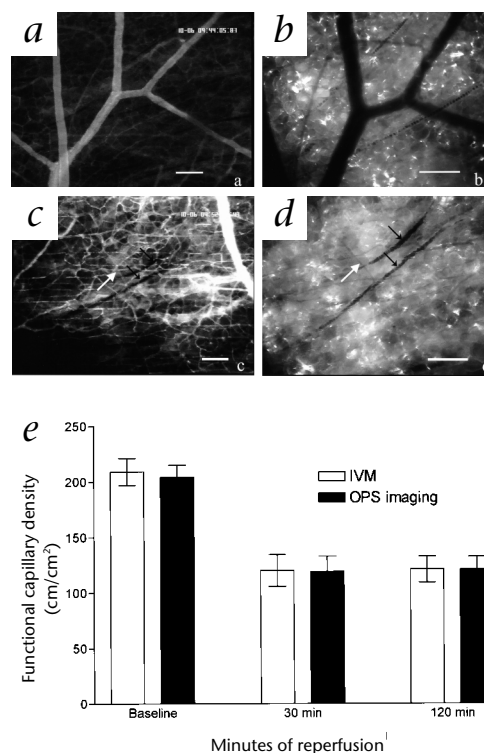


**Fig. 1** **a**, Orthogonal polarization spectral imaging probe. **b**, Optical schematic of the OPS imaging probe. A typical magnification of  $\times 10$  is maintained between the target and its image. This results in a resolution of approximately  $1 \mu\text{m}/\text{pixel}$ , which is limited by the dimension of the CCD pixel. The probe can be focused from the target surface to 1.0-mm depth, depending on the type of target and the optics used. *In vivo*, the typical depth of focus is approximately 0.2 mm. **c**, Optical

density of a graduated gray scale (catalog number 152-7662; Kodak) was measured in the presence of the polarization analyzer ( $\bullet$ ) or with a 0.5 OD neutral density filter ( $\circ$ ) used in place of the analyzer. Average light intensity for each gray level was converted to OD by the following formula:  $\text{OD} = \log_{10}((I_m - I_d)/(I_{\text{max}} - I_d))$  where  $I_m$  = measured light intensity,  $I_d$  = dark light intensity (obtained using a black velvet target),  $I_{\text{max}}$  = intensity of white target.

**Fig. 2** Images of the microcirculation dorsal skinfold preparation of the awake hamster taken during fluorescence intravital microscopy (**a** and **c**) and OPS imaging (**b** and **d**). Scale bar represents 100  $\mu\text{m}$ . In **a** and **b**, images were taken of the same microvascular network, demonstrating similar contrast in vessels imaged using fluorescence intravital microscopy and OPS imaging. In **c** and **d**, representative images are shown from the same animal, which were used for FCD measurements. The black arrows indicate two hair shafts that can be seen in both images showing it is the same capillary network. The white arrows indicate the same capillary in both images. Intravital fluorescence microscopy shows all capillaries filled with the fluorescent marker and OPS imaging shows those capillaries that are filled with red cells. Capillary flow cannot be seen in a static picture. However, during playback of the videotape, the moving RBCs in the capillaries can be seen clearly using OPS imaging or by following dark particles moving in the fluorescent network. **e**, Plot of functional capillary density measurements under baseline conditions ( $n = 60$ ), and after a 4-h pressure ischemia with 0.5 h of reperfusion ( $n = 60$ ) or 2 h of reperfusion ( $n = 60$ ). Data are shown as mean  $\pm$  s.d.



and its optical schematic are shown in Fig. 1a and b. To form the image, the light is collected, passed through a spectral filter to isolate the wavelength region, and linearly polarized. The polarized light is then reflected toward the target by a beam splitter. An objective lens focuses the light onto a region of approximately 1 mm in diameter. Light that is remitted from the target is collected by the same objective lens, which then forms an image of the illuminated region within the target upon a charge-coupled device (CCD) videocamera. The polarization analyzer is placed directly in front of the camera. A polarizing beam splitter is chosen for maximum efficiency. That is, one orthogonal polarization state is reflected while the other is transmitted.

In polarized light, the state of polarization of light is preserved in ordinary reflections as well as single scattering events. Typically, more than ten scattering events are required to depolarize light effectively<sup>9,10</sup>. Thus, the only remitted light from the subject that can pass through the analyzer results from multiple scattering occurring relatively deep (>10 times the single scattering length) within the medium. This depolarized scattered light effectively back-illuminates any absorbing material in the fore-

**Table 1** Comparison of contrast in epi-illumination between fluorescence-enhanced contrast and OPS imaging performed on paired images

Vessel diameter ( $\mu\text{m}$ )	Fluorescence contrast	OPS imaging contrast	Ratio
46	0.23	0.25	1.10
42	0.19	0.21	1.13
31	0.21	0.12	0.58
47	0.24	0.28	1.15
48	0.19	0.27	1.41
37	0.18	0.22	1.26
39	0.17	0.23	1.41
23	0.11	0.10	0.88
46	0.14	0.24	1.70
33	0.22	0.15	0.68
42	0.21	0.20	0.92
56	0.25	0.23	0.95
Average value	0.19	0.21	1.10
s.d.	0.04	0.06	0.32
n	12	12	12

Contrast is measured as the difference in intensity of the image at the vessel edge from the value at the center line divided by the sum of the intensity at the edge and at the center line. s.d., standard deviation.

ground. If a wavelength within the hemoglobin absorption spectrum is chosen, the blood vessels of the peripheral microcirculation can be visualized using OPS imaging as in transilluminated intravital microscopy. A wavelength region centered at an isobestic point (a wavelength at which both forms of hemoglobin absorb equally) of oxy- and deoxy-hemoglobin (548 nm) was chosen for optimal imaging of the microcirculation. This represented a compromise between using an isobestic point in the Soret region (about 420 nm), where hemoglobin absorption is maximum but the scattering length is shorter, or one in the near infrared region (810 nm), where multiple scattering occurs deep in the tissue but absorption for hemoglobin is insufficient to provide good contrast in smaller vessels.

Conventional reflectance spectrophotometry is carried out on an extended diffuse reflecting surface to which the analyte has been applied. Typically, reflectance spectrophotometry has a much more limited range of measurement of optical density (OD) than does transmission spectrophotometry, which can easily measure changes from 0 to 3 OD (see Fig. 1c). In reflected light spectroscopy, the apparent OD of the analyte is reduced by specular reflections and light scattering. The reflection and light scatter are due to physical characteristics rather than the chemical concentration of the analyte<sup>11</sup>. OPS imaging was developed in part to eliminate some of the confounding error inherent in reflectance spectroscopy that was due to reflection and light scatter. Figure 1c compares the OD measured using OPS imaging to reflectance spectrophotometry as a control. Measurements were made using a standardized gray-scale target. The optical path for the control system was identical to the OPS imaging optical train, except that a neutral density filter (0.5 OD) was substituted for the analyzer. In OPS imaging, the measurements obtained were linear over the OD range of 0 to 1.9 with a slope of 1.09, intercept of 0, and  $r^2$  of 0.999. In comparison, the control system became non-linear at 0.6 OD and had a useful spectrophotometric range of only 0.0 to 0.5 OD. The slope of the control system

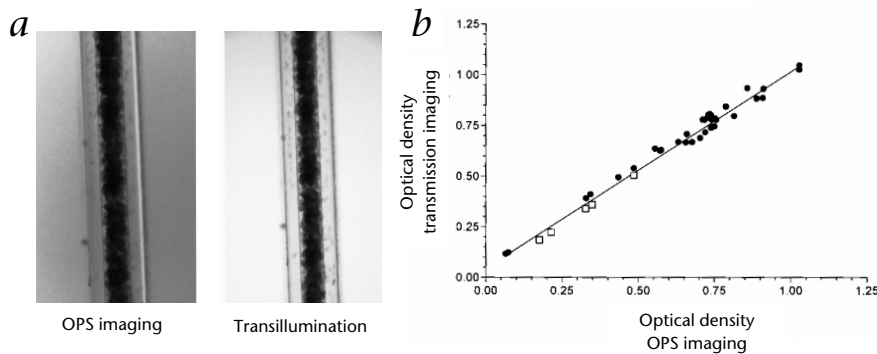


**Fig. 3** Quantitative determination of optical density *in vitro*. **a**, Capillary tubes (80- $\mu$ m square) filled with whole blood viewed using OPS imaging (reflected light) or transillumination. **b**, Correlation ( $r^2 = 0.984$ ) between OPS imaging and transillumination measurement of optical density in capillary tubes of either blood (●) or hemoglobin solutions (□). Optical density was determined from digital images obtained from the same probe during either OPS imaging or transmitted light imaging. During OPS imaging illumination, a thin Teflon disk was positioned behind the capillary tube to provide a surrogate tissue scattering medium for light reflection. For transmitted light imaging, a non-polarized light source of equal intensity to that observed during OPS imaging was positioned behind the capillary tube/Teflon disk target.

response (0.54) was approximately half of the OPS imaging system response. These results demonstrate that OPS imaging techniques can be used to accurately measure in reflection the wide range of OD typically achieved only in standard transmission spectrophotometry.

A theoretical explanation of OPS imaging includes the understanding that forming an image in reflected light requires both scattering for illumination and absorption for contrast. In continuous media, these are typically considered the result of a pair of material constants (coefficients)<sup>12</sup>. Both scattering and absorption depend linearly on penetration, and the remitted light intensity is given by the ratio of the coefficients<sup>11</sup>. High-quality imaging is therefore generally not possible in turbid media because of the scattering, which degrades the image resolution. However, in OPS imaging, the remitted illumination is provided only by multiple scattering. This is a distinctly non-linear function of the penetration depth and thus is decoupled from the absorption. Consequently, absorbing substances at shallow depth can be visualized with both high contrast and good resolution.

#### Comparison with *in vivo* intravital microscopy

The ability of OPS imaging to provide quantitative measurements of relevant physiological parameters and pathophysiological changes in the microcirculation was shown by measurement of functional capillary density (FCD) in the dorsal skinfold chamber of the awake Syrian golden hamster<sup>13,14</sup>. FCD is defined as the length of red blood cell (RBC)-perfused capillaries per observation area and is given in  $\text{cm}/\text{cm}^2$ . As the capillaries must contain flowing red cells to be counted in the measurement,

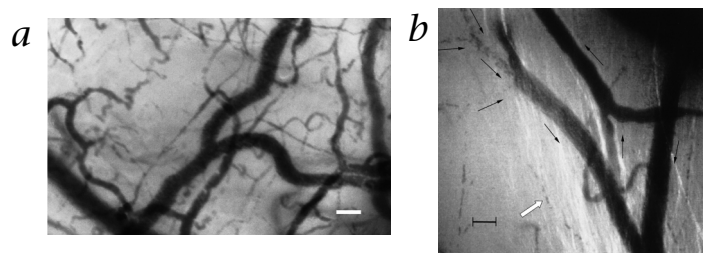
site in each animal. As the measurement of FCD is a dynamic event, not all capillaries can be clearly seen in the static images, although some typical capillary structures can be seen. Thus, although one may actually see many capillaries in the picture that are filled with the fluorescent dye (see Fig. 2a and c), this does not necessarily mean that they will be counted in the FCD measurement, unless a RBC (in this case a small dark spot) can be seen moving through it. Figures 2c and d show a representative network used for FCD measurements. After postischemic reperfusion, FCD was measured equally well by the two imaging methods (Fig. 2e). As has been demonstrated in this preparation<sup>13</sup>, there was a decrease in capillary perfusion (of about 60%). Furthermore, Bland-Altman analysis<sup>16</sup> showed very good agreement between methods, as well as no systematic bias over the entire range of FCD measurements.

A direct comparison was made of the contrast between OPS imaging and fluorescence on paired images of the hamster dorsal skinfold microcirculation (Fig. 2a and b). Twelve blood vessels were chosen for this analysis, ranging in diameter from 23 to 56  $\mu$ m. There was no significant difference between the two methods in absolute contrast (Table 1;  $P = 0.43$ , paired *t*-test). Thus, contrast obtained by OPS imaging without the use of dyes was equivalent to that obtained with contrast enhancement by fluorescence.

#### Quantitative determination of optical density *in vitro*

Quantitative data regarding local hematocrit, which can be obtained with transillumination using the absorbance of blood hemoglobin, is not possible using epi-illumination methods

**Fig. 4** OPS images of human microcirculation. **a**, Sublingual microcirculation. OPS images obtained from a probe placed gently under the tongue. Scale bar represents 100  $\mu$ m. **b**, Pial microcirculation before brain surgery. Moving single erythrocytes can be observed ( $\Rightarrow$ ) as they flow in single file through the capillaries, into venules and into larger veins. The dark arrows indicate the direction of blood flow and the measurement bar length equals 90  $\mu$ m.



## Methods

**Intravital microscopy.** Hamster dorsal skinfold chambers and the surgical implantation procedure used in this study have been described in detail<sup>13</sup>. The setup and microscope system used to make the fluorescent videomicroscopy measurements has been presented in a recent publication<sup>14</sup>. Fluorescein isothiocyanate-labeled dextran (FITC-dextran, 0.05 ml, 3%, M<sub>w</sub> = 150,000; Sigma) was used for contrast enhancement of the microvessels for fluorescence microscopy measurements. To take advantage of the computer-controlled microscope functions, the OPS imaging probe was attached to the shaft of the microscope using a specially designed C-clamp. The Plexiglas stage was modified so that there were two different pairs of holes, with which the stage could be attached to the motorized plate. One pair of holes aligned the chamber under the fluorescence microscope and the other set aligned the chamber under the OPS imaging probe. Moving the stage from one pair of holes to the other allowed the identical region of interest to be seen with the two systems. In five of the animals, the fluorescence microscopy measurements were made first and in the other five animals OPS imaging measurements were made first to assure that no bias was introduced as a result of the measurements being made consecutively and not simultaneously.

**Functional capillary density.** For the measurement of FCD, six regions of interest were selected, their positions stored on the computer, and the baseline measurements were made with both systems in a randomized order. For each measurement the capillary beds were videotaped for 30 s with each of the systems. The chamber tissue was then subjected to a 4-h pressure ischemia<sup>23</sup>. The observation procedure was repeated 0.5 h and 2 h after reperfusion. The images from both systems

without fluorescent labeling of the red cells. Previous studies to determine local hematocrit using intravital microscopy used thin tissue sections (such as the rat mesentery or cremaster muscle<sup>17</sup>). The optical systems used for those studies were evaluated and calibrated using glass capillaries filled with solutions of hemoglobin and/or whole blood<sup>18,19</sup>. We demonstrate that the OPS imaging system produces images of blood-filled capillary tubes similar to those obtained by transillumination (Fig. 3a). The optical densities obtained from transillumination and OPS imaging were compared for a series of measurements made on glass capillaries filled with diluted whole blood or solutions of hemoglobin. The receiving optics were identical. The optical densities were essentially identical ( $r^2 = 0.984$ ; Fig. 3b). Thus, OPS imaging can be useful in the quantitative determination of local hematocrit using the optical density approach in epi-illumination.

OPS imaging relies on the absorbance of hemoglobin to create contrast. Thus, the vessel must contain RBCs to be visualized. For measurement, the vessel needs to be greater in diameter than the minimum resolution of the camera and optics. For these particular images, the magnification at the camera was one micrometer per pixel. Therefore, the resolving power of the system was sufficient to resolve a single RBC and individual capillaries of approximately 5  $\mu\text{m}$  in diameter. Finally, there must be sufficient contrast between RBCs and the surrounding tissue. Small vessels corresponding to capillaries can be seen easily (Fig. 2c and d). However, the appearance of single-file RBC flow and large plasma spaces in these smaller vessels often results in vessel segments that have relatively few RBCs. Errors in diameter measurement are more likely in smaller vessels because of streaming of the RBCs in the center of the vessel and cell packing. Thus, although RBCs, blood flow and diameters of these vessels are easily visualized, and FCD can be measured, we have not made attempts to measure optical density in vessels smaller than 10  $\mu\text{m}$ .

were analyzed during repetitive playback using a computer-assisted microcirculation analysis system (Cap-Image; H. Zeintl, Heidelberg, Germany)<sup>20</sup> and FCD was determined using the images from both methods. FCD is assessed as the length of RBC-perfused capillaries per observation area and is given in  $\text{cm}/\text{cm}^2$ . The measurement is made by watching the 30-second clip of the microvascular network repeatedly and, using a computer mouse, tracing out the length of all capillaries that have RBCs flowing through them. If only a single RBC traverses a capillary during the observation period, this capillary is included in the measurement.

**OPS imaging during surgery.** The OPS imaging probe, videorecorder, monitor and video printer were connected to an isolation transformer. The parts that came into physical contact with the patient were sterilized before surgery. To allow the surgeon to position the light guide on the brain surface and to hold the image guide in place for stable video recordings, a stainless steel surgical arm with three pivot points was used. The arm could be made rigid by twisting a number of securing knobs. This was built at the Academic Medical Center (AMC) of the University of Amsterdam and tested and certified for safety by the Department of Medical Instrumentation for use solely at the AMC. Permission for use of this device during brain surgery was obtained from patients and the Medical Ethical Committee of the AMC. Before surgery, the arm with the OPS imager was secured to the rails of the operating table. The arm was covered by sterile foil used for covering endoscopes, which in turn was attached to the sterile Teflon sleeve covering the light guide. After craniotomy, the imager was gently positioned on the surface of the pia mater. The surgeon could see the microcirculation of the brain on the TV monitor.

## OPS imaging of human microcirculation

Intravital imaging by transmission microscopy is not possible in humans or animals for inaccessible sites or solid organs. The OPS imaging method uses a small-sized probe and produces clear images of the microcirculation by reflectance from the surface of solid organs and from sites such as the sublingual area in the awake human. The image in Fig. 4a was obtained by placing the OPS imaging probe under the tongue as one would place an oral thermometer. OPS imaging could thus show differences between normal and pathological microvascular structure and function non-invasively. The diagnosis and progression of disease and the effectiveness of treatment could be monitored for disorders in which altered microvascular function has been found.

Using a specially prepared OPS imaging device, we have imaged the pial circulation in anesthetized humans just before neurosurgery (Fig. 4b). Although it is difficult to see in a static image, during video playback, RBCs could be seen flowing in single file through capillaries. Vessels could be readily identified as arterioles, capillaries or venules. Video images were of sufficient quality to allow quantification of red-cell flux using commercially available image processing software originally developed for analysis of video images obtained from intravital microscopy<sup>20</sup>. We have obtained equally informative images of other human microcirculatory beds in the esophagus and the stomach.

## Additional applications

Additional applications of OPS imaging, originally described by Winkelman<sup>21</sup>, are to use images of the microcirculation to measure directly and compute key elements of the complete blood count. The combination of OPS imaging, image processing, reflectance spectroscopy and algorithmic calculation, can yield a rapid determination of hemoglobin concentration, hematocrit and white blood-cell count without withdrawing blood samples from the body. Non-invasive blood testing will have substantial

utility in medical practice. Further applications of OPS imaging may include improved analytic reflection spectrophotometry similar to the quantitative dipstick methods used to determine analytes in urine<sup>22</sup> *in vitro* on paper strips.

### Implications and future directions

OPS imaging technology will provide new diagnostic tests for human microvascular pathologies. The small size of the probe will facilitate its use as a non-invasive diagnostic tool in both experimental and clinical settings to evaluate and monitor the microvascular sequelae of conditions known to affect the microcirculation, such as shock (hemorrhagic, septic), hypertension or diabetes. In addition to non-invasive applications, imaging and quantitative analysis of the microcirculation during surgery (transplant, cardiac, vascular, neurological, plastic, etcetera), wound healing, tumor therapy and intensive care medicine are being evaluated. The ability to obtain high-contrast images of the human microcirculation using reflected light will allow quantitative determination of parameters such as capillary density, microvessel morphology and vascular dynamics at many previously inaccessible sites. These measurements will be essential in developing precise tools to evaluate perfusion during clinical treatment of those diseases that impact tissue viability and microvascular function. Using this methodology, physicians may now be able to follow the progression and development of microvascular disease and directly monitor the effects of treatment on the microcirculation.

### Acknowledgments

We thank A. Loeb, G. Fletcher, C. Cook, A. Perkins, R. Pittman and R. Johnson for discussions and critically reviewing the manuscript. These studies were funded in part by Cytometrics.

- Forst, T. *et al.* Skin microcirculation in patients with type I diabetes with and without neuropathy after neurovascular stimulation. *Clin. Sci.* **94**, 255–261 (1998).
- Fagrell, B. & Bollinger, A. in *Clinical Capillaroscopy: A Guide to Its Use in Clinical Research and Practice* (Hogrefe & Huber, Seattle, Washington, 1990).
- Fagrell, B. & Intaglietta, M. Microcirculation: Its significance in clinical and molecular medicine. *J. Int. Med.* **241**, 349–362 (1997).
- Davis, E. & Landau, J. in *Clinical Capillary Microscopy* (Thomas, Springfield, Illinois, 1966).
- Fenton, B.M., Zweifach, B.W. & Worthen, D.M. Quantitative morphometry of conjunctival microcirculation in diabetes mellitus. *Microvasc. Res.* **18**, 153–166 (1979).
- Wolf, S., Arend, O., Schulte, K., Ittel, T.H. & Reim, M. Quantification of retinal capillary density and flow velocity in patients with essential hypertension. *Hypertension* **23**, 464–467 (1994).
- Bussau, L.J. *et al.* Fibre optic confocal imaging (FOCI) of keratinocytes, blood vessels and nerves in hairless mouse skin *in vivo*. *J. Anat.* **192** (Pt. 2), 187–194 (1998).
- Rajadhyaksha, M., Grossman, M., Esterowitz, D., Webb, R.H. & Anderson, R.R. *In vivo* confocal scanning laser microscopy of human skin: Melanin provides strong contrast. *J. Invest. Dermatol.* **104**, 946–952 (1995).
- MacKintosh, F.C., Zhu, J.X., Pine, D.J. & Weitz, D.A. Polarization memory of multiply scattered light. *Phys. Rev. B* **40**, 9342 (1989).
- Schmitt, J.M., Gandjbakhche, A.H. & Bonner, R.F. Use of polarized light to discriminate short-path photons in a multiply scattering medium. *Appl. Opt.* **31**, 6535 (1992).
- Kortüm, G. in *Reflectance Spectroscopy* (Springer-Verlag, New York, 1969).
- Star, W.M., Marijnissen, J.P.A. & van Gemert, M.J.C. Light dosimetry in optical phantoms and in tissues: I. Multiple flux and transport theory. *Phys. Med. Biol.* **33**, 437–454 (1988).
- Harris, A.G., Leiederer, R., Peer, F. & Messmer, K. Skeletal muscle microvascular and tissue injury after varying durations of ischemia. *Am. J. Physiol.* **271**, H2388–2398 (1996).
- Harris, A.G., Hecht, R., Peer, F., Nolte, D. & Messmer, K. An improved intravital microscopy system. *Int. J. Microcirc. Clin. Exp.* **17**, 322–327 (1997).
- Nolte, D., Zeintl, H., Steinbauer, M., Pickelmann, S. & Messmer, K. Functional capillary density: An indicator of tissue perfusion? *Int. J. Microcirc. Clin. Exp.* **15**, 244–249 (1995).
- Bland, J.M. & Altman, D.G. Statistical methods for assessing agreement between two methods of clinical measurement. *Lancet* **i**, 307–310 (1986).
- Pittman, R.N. & Duling, B.R. Measurement of percent oxyhemoglobin in the microvasculature. *J. Appl. Physiol.* **38**, 321–327 (1975).
- Pittman, R.N. & Duling, B.R. A new method for the measurement of percent oxyhemoglobin. *J. Appl. Physiol.* **38**, 315–320 (1975).
- Lipowsky, H.H., Usami, S., Chien, S. & Pittman, R.N. Hematocrit determination in small bore tubes by differential spectrophotometry. *Microvasc. Res.* **24**, 42–55 (1982).
- Klyszcz, T., Jünger, M., Jung, F. & Zeintl, H. Cap image—a new kind of computer-assisted video image analysis system for dynamic capillary microscopy. *Biomed. Tech. (Berlin)* **42**, 168–175 (1997).
- Winkelmann, J.W. Apparatus and method for *in vivo* analysis of red and white blood cell indices. US Patent 4998553 (1991).
- Peele, J.D., Gadsen, R.H. & Crews, R. Evaluation of Ames' "Clini-Tek." *Clin. Chem.* **123**, 2238–2241 (1977).
- Nolte, D., Menger, M.D. & Messmer, K. Microcirculatory models of ischaemia-reperfusion in skin and striated muscle. *Int. J. Microcirc. Clin. Exp.* **15**, 9–16 (1995).

## ON THE MARKET

### ASSORTED ANTIBODIES

TCS Biologicals offers Upstate Biotechnology's novel **antibody to a receptor involved in pain and drug addiction**—a polyclonal antibody to kappa opioid receptor (KOR-1). KOR-1 receptors have been shown to be one of the receptors involved in binding products resulting from morphine metabolism. Excessive exposure to such agonists leads to desensitization of the receptors and the need for higher doses of drug to obtain the same results. The possible implication of this receptor in drug addiction and pain control makes it a useful target for future research. The antibody is suitable for immunoblots, immunoprecipitation and immunohistochemistry studies.

**Reader Service No. 92**

**Tel. (+44) (0) 1296-714071**

**Fax (+44) (0) 1296-715753**

BABCO has introduced **monoclonal antibodies that are specific for four synaptic markers**: SNAP-25, synaptophysin, synaptobrevin and syntaxin. All four antibodies have been shown to react with human, rat, pig and hamster samples (anti-SNAP-25 also reacts with cat). These antibodies can be used for immunoblotting and ELISAs, and are said to be particularly applicable for immunocytochemical studies of the brain as the recognized epitopes are stable in the presence of formalin.

**Reader Service No. 93**

**Tel. (+1) 510-412-8930**

**Fax (+1) 510-412-8940**

AutoGen Bioclear now offers the QCB range of  **$\beta$ -amyloid research products** in addition to its own neurochemicals and products for Alzheimer's disease research. Three new fluorescent ELISA kits for the detection of A $\beta$ 1-40, A $\beta$ 1-42 and

A $\beta$ 1-43 can detect  $\beta$ -amyloid from samples containing as little as 10 pg/ml of the target peptide. Polyclonal antibodies to A $\beta$ 1-40, A $\beta$ 1-42 and A $\beta$ 1-43,  $\beta$ -secretase site-specific (A $\beta$  N-terminal) and monoclonals to A $\beta$ 1-16, A $\beta$ 17-26 and A $\beta$ 18-28 are available, in addition to over 45 bioactive  $\beta$ -amyloid peptides and protein precursors, some of which are conjugated to biotin and fluorescein.

**Reader Service No. 94**

**Tel. (+44) (0) 1249-819008**

**Fax (+44) (0) 1249-817266**

### PATCH CLAMPING

Burleigh Instruments is offering the new Gibraltar **platform and x,y, stage** as a compliment to its PCS-5000 range of micromanipulators. These new additions are said to provide a rock-steady platform for researchers undertaking multiple patching experiments. Fully height adjustable and offering precise control